

Magnetic Roughness and Domain Correlations in Antiferromagnetically Coupled Multilayers

Sean Langridge and Jörg Schmalian

Rutherford Appleton Laboratory, Chilton, Didcot, Oxfordshire, OX11 0QX, United Kingdom.

C.H. Marrows, D.T. Dekadjevi and B.J. Hickey

Department of Physics and Astronomy, E.C. Stoner Laboratory, University of Leeds, Leeds, LS2 9JT, United Kingdom.

(October 11, 2018)

The in-plane correlation lengths and magnetic disorder of magnetic domains in a transition metal multilayer have been studied using neutron scattering techniques. A new theoretical framework is presented connecting the observed scattering to the in-plane correlation length and the dispersion of the local magnetization vector about the mean macroscopic direction. The results unambiguously show the highly correlated nature of the antiferromagnetically coupled domain structure vertically throughout the multilayer. We are easily able to relate the neutron determined magnetic dispersion and domain correlations to magnetization and magnetotransport experiments.

75.25.+z, 75.50.Cn, 75.70.Pa

The interplanar coupling and in-plane magnetic domains are essential to an understanding of the origin of the large giant magnetoresistance effect (GMR) [1] in magnetically coupled multilayers. This coupled with the advances in thin film deposition techniques [2] has led to a huge interest in magnetic multilayer systems specifically with respect to their device application possibilities. The GMR effect arises from the antiferromagnetic (AF) coupling of typically a transition metal ferromagnet (e.g. Co) across a noble metal non-magnetic spacer (e.g. Cu). This AF coupling can be realized by tuning the noble metal spacer thickness [3]. The change in resistivity results from the spin dependent scattering of the conduction electrons which depends not only on the magnetic moment alignment but also on the interfacial disorder [4] and the magnetic domain structure. Until recently the question of the relationship between magnetic domain structure and interlayer coupling has not been explored experimentally. It is clear that a vertically incoherent magnetic domain structure will have the effect of lowering the GMR by preventing perfect AF alignment in adjacent layers [5]. In studies of a weakly coupled system such as $[\text{Cu}(60\text{\AA})/\text{Co}(60\text{\AA})] \times 20$ it was shown that the reduction in the GMR from the as-prepared state to the coercive state can be understood as a loss of vertical coherence of the AF coupling [6]. The situation is different in the strongly coupled samples investigated here, the results of which clearly show magnetically correlated domains at the coercive field which extend vertically throughout the entire multilayer.

The investigation of *structurally* rough interfaces is well established and makes use of diffuse x-ray scattering techniques. The theoretical tools for analyzing various surface morphologies are well advanced [7–10]. Recent advances in x-ray techniques have applied this structural formalism to the study of magnetically rough systems [11–17]. Nevertheless, the problem of quantifying magnetic roughness remains difficult primarily due to the indirect and complicated nature of the spin-photon interaction [18,19]. This problem can be resolved by neutron techniques for which the direct interaction between the neutron's dipole moment and the sample magnetization is well understood.

In this letter we have performed neutron scattering measurements on magnetically coupled multilayers and quantitatively determined the field dependence of the magnetic roughness and domain distribution. The large lateral coherence length of the neutron beam ($> 30\mu\text{m}$ [20]) ensures that the measurements sample many magnetic domains. Since the neutrons are highly penetrative the measurements also sample the whole multilayer vertically, unlike the transition metal L_{III} x-ray measurements [21] which sample primarily the uppermost interfaces because of the high x-ray absorption coefficient.

We prepared Co/Cu and Co/Ru multilayers of 50 bilayer repeats, with Cu and Ru spacer thicknesses corresponding to the 1st and 2nd AF maxima of the coupling oscillation, for different thicknesses of the magnetic layer. The samples were deposited by dc magnetron sputtering in a custom vacuum system with a base pressure of 2×10^{-8} Torr. The multilayers were grown on 20 mm \times 25 mm pieces of (001) Si wafer with the native oxide layer left intact. The working gas was 3 mTorr of Ar, and deposition rates for Co, Cu and Ru were all $\sim 3 \text{ \AA/s}$. Smaller 10 mm \times 2 mm samples were grown in the same growth run for magnetoresistance and Magneto-Optic Kerr Effect (MOKE) measurements.

The reflectivity measurements, both polarized and non-polarized, were performed on the time-of-flight polarized neutron beam reflectometer CRISP at the ISIS facility, Rutherford Appleton Laboratory [22,23]. To maximize the flux at the sample position, for the diffuse scattering measurements, the reflectometer was run in a non-polarized mode with an incident wavelength range of 0.5 \AA –6.5 \AA . An electromagnet at the sample position provides an in-plane

reversible field of ± 7 kOe. The scattered neutrons are detected by a 1-dimensional ${}^3\text{He}$ detector. The combination of the time-of-flight technique and the multidetector ensure that both the parallel (Q_Z) and perpendicular (Q_X) (to the surface normal) components of the neutron wave-vector transfer (see fig 1) are obtained in a single measurement. Typical acquisition times are of the order of 2 hours for an entire reciprocal space map, which compares favorably with resonant x-ray techniques [21].

Fig.1(a) presents the observed reciprocal space intensity map for the nominal $[\text{Co}(20\text{\AA})/\text{Cu}(20\text{\AA})] \times 50$ multilayer at remanence. This Cu thickness corresponds to the 2nd AF ordering peak. Although we have similar data for other Co, Cu and Ru layer thicknesses we shall concentrate on this sample in this article. Three features are apparent in the data: the specularly reflected ridge ($Q_X=0 \text{ \AA}^{-1}$), the first order nuclear Bragg peak ($Q_Z=0.15 \text{ \AA}^{-1}$) and the Bragg peak corresponding to the AF periodicity ($Q_Z=0.075 \text{ \AA}^{-1}$). This peak is entirely magnetic in origin. The first order Bragg peak indicates that the bilayer thickness is $\sim 42 \text{ \AA}$. The narrow width in Q_Z (see inset) implies that the AF order is coherent throughout the whole multilayer.

A major conclusion of this paper results from the comparison of the Q_X distribution of the two peaks. The nuclear Bragg peak is sharp but the AF peak is diffuse. The roughness is therefore predominantly magnetic. We associate this magnetic roughness with the existence of AF coupled domains. The diffuse scattering is strongly peaked in Q_Z therefore our data gives evidence for the coherent coupling of the magnetic domains vertically through the multilayer. Note, no evidence for diffuse scattering from uncorrelated regions was observed which would be uniformly distributed in Q_Z [24]. Applying a saturating field (Fig.1(b)) destroys the AF correlations resulting in a ferromagnetic alignment. Fig.2 details sections in Q_X through the AF Bragg peak as one cycles from close to remanence to positive saturation and then reverse to negative saturation. At low fields (< 100 Oe) the scattering is dominated by the diffuse scattering. As the field is increased to saturation only the specular ridge remains. Equivalent sections through the nuclear Bragg peak reveal no evidence of diffuse scattering.

In order to quantitatively analyze our data and to characterize the domain structure of the multilayer system, we now present a new theoretical framework for diffuse magnetic scattering in systems with a spatially inhomogeneous magnetization profile, $\mathbf{m}(\mathbf{r})$, where \mathbf{r} is the position vector. Considering a system where $\mathbf{m}(\mathbf{r})$ is in-plane, we can write $\mathbf{m}(\mathbf{r}) = m_0(\cos \phi(\mathbf{r}), \sin \phi(\mathbf{r}), 0)$, with phase angle, $\phi(\mathbf{r})$, and amplitude, m_0 . Thus, we consider solely directional variations of $\mathbf{m}(\mathbf{r})$ which describe the different orientations of the magnetic domains. We treat $\mathbf{m}(\mathbf{r})$ and therefore $\phi(\mathbf{r})$ as random variables, characterized by the correlation function $C(|\mathbf{r}|) = \langle \phi(\mathbf{r})\phi(0) \rangle$. This is similar to the treatment of structurally rough surfaces by Sinha *et al.* [7]. Thus, $\phi(\mathbf{r})$ plays a role reminiscent to the local height variation in the non-magnetic case and we parametrize $C(r)$ as:

$$C(r) = \sigma^2 \exp(-r/\xi) . \quad (1)$$

$\sigma = \langle \phi^2 \rangle$ is the width of the angular distribution and therefore characterizes the *local magnetic roughness*. ξ is the lateral correlation length, i.e. a measure for a typical domain size. We consider the magnetic scattering function within the Born approximation, $S(\mathbf{Q}) \propto \sum_{\alpha\beta} \int d^3\mathbf{r} e^{i\mathbf{Q}\cdot\mathbf{r}} \left(\delta_{\alpha\beta} - \hat{Q}_\alpha \hat{Q}_\beta \right) \langle m_\alpha(\mathbf{r})m_\beta(0) \rangle$, where \hat{Q}_α is a unit vector component of the transferred momentum, \mathbf{Q} . Performing the average with respect to the different domain orientations by assuming a Gaussian distribution for $\phi(\mathbf{r})$, we find in addition to the specular scattering, $S_{\text{spec.}}(\mathbf{Q}) = m_0^2 e^{-\sigma^2} \delta(\mathbf{Q}_{\parallel})$, the diffusive scattering function:

$$S_{\text{diff.}}(\mathbf{Q}) = m_0^2 e^{-\sigma^2} \int d^2\mathbf{r} e^{i\mathbf{Q}_{\parallel}\cdot\mathbf{r}} \left[(1 - \hat{Q}_X^2) \sinh(C(r)) + (1 - \hat{Q}_Y^2) 2 \sinh^2(C(r)/2) \right] . \quad (2)$$

Here, \mathbf{Q}_{\parallel} is the in-plane component of \mathbf{Q} . In our experimental geometry the detector aperture is set up such that the neutron intensity is integrated out over Q_Y , which is parallel to the applied field. Finally, when evaluated at the AF ordering vector, it holds that $m_0 = \mu \sin(\theta/2)$, where μ is the Co magnetic moment and θ the angle between Co moments in adjacent layers. Before we analyze our data using Eq. 2 we emphasize that, within the Gaussian approximation, we treat the angle $\phi(\mathbf{r})$, normally restricted to $\pm\pi$, as an unrestricted variable. Therefore, we cannot describe a system with equally distributed angles, i.e. with $\langle e^{i\phi(\mathbf{r})} \rangle = 0$. However, this practically never occurs after the system was exposed to an external field, even if this field is set to zero or equal to the coercive field, see also our results in Fig. 2, where the AF peak always has some specular component. Furthermore, our result for the diffusive magnetic scattering, Eq. 2, is anisotropic with respect to Q_x and Q_y . This is because magnetic fluctuations perpendicular to the field are not only larger in amplitude but also more extended in space compared to those parallel to the field. In the present scattering geometry this effect is negligible since $Q_x^2, Q_y^2 \ll Q_z^2 \approx 1$. However, for smaller

Q_z or by using polarized neutrons, we predict a pronounced anisotropy of the diffuse magnetic scattering if $S(\mathbf{Q})$ is averaged with respect to the component of \mathbf{Q} parallel or perpendicular to the field.

The results of numerically convoluting the specular and diffuse (Eq.2) contributions with the instrumental resolution function and performing a least-squares fit to the data are shown in Fig. 3. The agreement between theory and experiment is excellent. Panels (a) and (b) display the observed magnetization loop as measured by MOKE measurements and the normalized change in resistivity respectively. The MOKE loop and magnetoresistance curve both indicate good AF coupling. For fields close to remanence the Co layers have a global anti-parallel alignment(c) with a large magnetic roughness(d) and a characteristic domain size of $\approx 1\mu\text{m}$. For increasing fields three effects occur. The anti-parallel alignment across the non-magnetic spacer is diminished. The orientational domain distribution within a given layer focuses around the applied field direction and the domain size increases to $\approx 7\mu\text{m}$. Even at reasonably large fields the moments are not perfectly aligned about the field direction. At $+200$ Oe there still remains a substantial domain distribution although the orientation of adjacent layers is nearly ferromagnetic ($m_0 \rightarrow 0$). At these fields the diffuse scattering approaches the experimental background (primarily from incoherent scattering) and represents the limits of the current measurements. For this reason we cannot measure values of σ close to zero in Fig. 3 as saturation is approached. At saturation only the structural specular peak remains. The data clearly show the hysteresis in moving around the loop. The fact that all quantities in Fig. 3 follow this hysteresis loop reveals the close correlation between the GMR effect and the magnetic domain correlations. The decrease of the angle θ between the magnetization in neighboring layers causes not only the expected decrease of the GMR but also a decreasing roughness accompanied by an increase of the domain size. The latter effect is particularly drastic for fields above the coercive field, H_c , i.e. $\xi \approx \xi_0 f(H/H_c)$ with non-linearly growing function $f(x)$. Below H_c the dominant effect is the focusing of domain orientations. The observed increase in domain size from $\sim 1.5\mu\text{m}$ to $7\mu\text{m}$ extracted from the data is typical of such systems [25,26]. Interestingly, qualitatively similar effects have been observed around the nuclear/ferromagnetic Bragg peak for an equivalent ferromagnetically coupled system.

We now turn to the domain reversal mechanism. This can take place by directional magnetization fluctuations which are focused by the applied field. or by domain wall motion where the axis of magnetization is unchanged due to a dominating magneto-crystalline anisotropy. In this latter scenario σ would be a measure for the probability of the magnetization aligning anti-parallel to the external field rather than the width of a directional distribution. However, our samples are only weakly anisotropic. Imaging of 2nd AF coupled multilayers [29] strongly supports a domain reversal predominantly via rotation of the magnetization in agreement with our analysis.

Our results can be compared with the recent work of Borchers *et al.* (Ref. [6]) on a weakly coupled system. Their data show that the reduction in the GMR from the as-prepared state to the coercive state can be understood as a loss of coherence of the AF coupling. The more strongly coupled samples investigated here clearly show magnetically correlated domains at the coercive field. By increasing the exchange coupling by replacing Cu with Ru [27] there is a significant change in the domain structure. Even at remanence the correlation length is $\xi = (7 \pm 3) \times 10^4 \text{ \AA}$, with the diffuse tail extending across the whole of the Q_X range. It is important to note that only with the very long lateral coherence lengths of the neutron beam used is it possible to measure ξ accurately when it is so large. A full discussion of the dependence on spacer material and magnetic and spacer layer thicknesses will be published separately [28].

To summarize, within a new theoretical framework we have quantified the magnetic domain structure in an AF coupled multilayer using diffuse magnetic neutron scattering. The systematic study of the field dependence of the diffuse scattering reveals a close relationship between magnetic roughness, domain size, interlayer coupling and the GMR effect itself.

ACKNOWLEDGMENTS

The authors gratefully acknowledge fruitful discussions with J.R.P. Webster, J. Penfold, S.W. Lovesey and S.K. Sinha. C. H. Marrows would like to thank the Royal Commission for the Exhibition of 1851 for financial support. We are grateful to the Rutherford Appleton Laboratory for the provision of ISIS beamtime.

[1] M.N. Baibach *et al.*, Phys. Rev. Lett. 61, 2472 (1988)
[2] D. L. Smith, Thin-Film Deposition: Principles and Practice, McGraw-Hill, New York (1995)

- [3] S. S. P. Parkin, N. More and K. P. Roche, Phys. Rev. Lett. **64**, 2304 (1990); S. S. P. Parkin, R. Bhadra, and K. P. Roche, Phys. Rev. Lett. **66**, 2152 (1991)
- [4] P. Zahn *et al.* Phys. Rev. Lett. **80**, 4309 (1998)
- [5] H. Holloway and D. J. Kubinski, J. Appl. Phys. **83**, 2705 (1998)
- [6] J.A. Borchers *et al.*, Phys. Rev. Lett. **82**, 2796 (1999)
- [7] S.K. Sinha *et al.*, Phys. Rev. B **38**, 2297 (1988)
- [8] S.K. Sinha *et al.*, Physica B **198**, 72 (1994)
- [9] V. Holý *et al.*, Phys. Rev. B **49**, 10668 (1994)
- [10] R. Pynn, Phys. Rev. B **45**, 602 (1992)
- [11] C.T. Chen *et al.*, Phys. Rev. B. **48**, 642 (1993).
- [12] J.W. Freeland *et al.*, J. Appl. Phys. **83**, 6290 (1998)
- [13] Y.U. Idzerda *et al.*, Phys. Rev. Lett. **82**, 1562 (1999)
- [14] J.F. MacKay *et al.*, Phys. Rev. Lett. **77**, 3925 (1996)
- [15] C. Kao *et al.*, Phys. Rev. Lett. **65**, 373 (1990)
- [16] P. Fischer *et al.*, J. Phys. D. **31**, 645 (1998).
- [17] V. Chakrian *et al.*, Appl. Phys. Lett. **66**, 3368 (1995)
- [18] D. Gibbs *et al.*, Phys. Rev. Lett. **61**, 1241 (1988)
- [19] J.P. Hannon *et al.*, Phys. Rev. Lett. **61**, 1245 (1988)
- [20] J.R.P. Webster, private communication (1999)
- [21] T.P.A Hase, PhD Thesis, University of Durham (1998)
- [22] R. Felici *et al.*, Appl. Phys. A **45**, 169 (1988)
- [23] <http://www.isis.rl.ac.uk/largescale/crisp/CRISP.htm>
- [24] D.E. Savage *et al.*, J. Appl. Phys. **69**, 1411 (1991)
- [25] L. J. Heyderman, J. N. Chapman, and S. S. P. Parkin, J. Phys. D: Appl. Phys. **27**, 881 (1994)
- [26] M. Herrman, S. McVitie, J. N. Chapman, C. H. Marrows and B. J. Hickey (unpublished)
- [27] S. S. P. Parkin, Phys. Rev. Lett. **67**, 3598 (1991)
- [28] S. Langridge, C. H. Marrows and B. J. Hickey, unpublished.
- [29] P. Aitchison, J. N. Chapman, D. B. Jardine, and J. E. Evetts, J. Appl. Phys. **81**(8)Pt.2A, 3775 (1997)

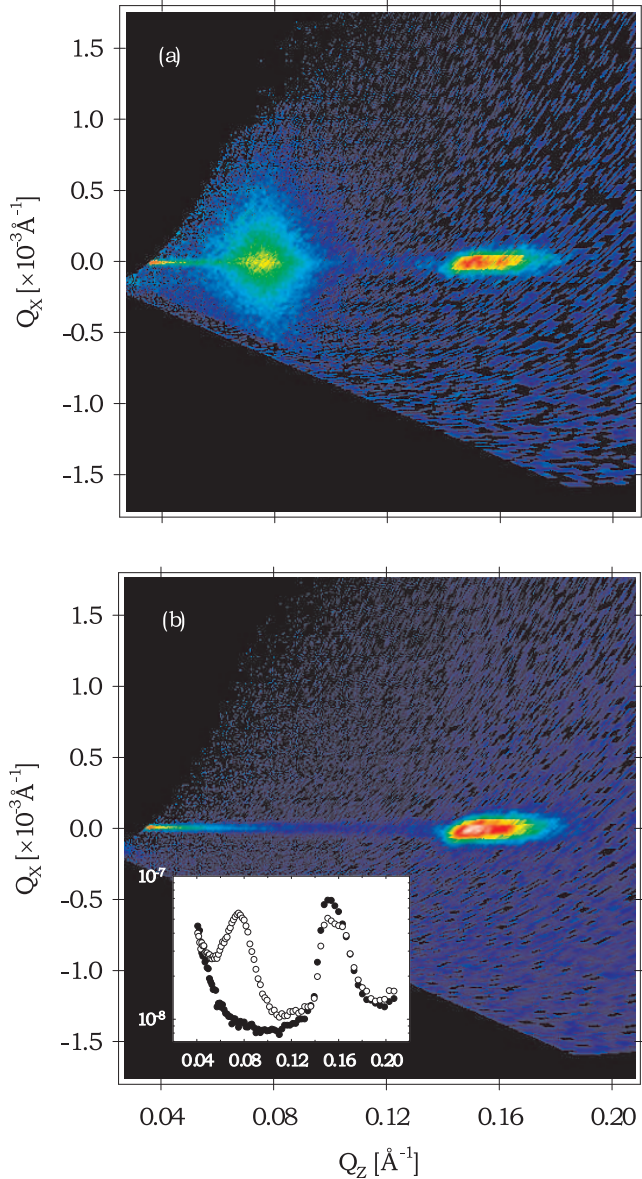


FIG. 1. (a): The observed scattering from the $[\text{Co}(20\text{\AA})/\text{Cu}(20\text{\AA})] \times 50$ multilayer in zero applied field. The intensity centered at $Q_z = 0.075 \text{ \AA}^{-1}$ corresponds to the AF ordering wave-vector and arises purely from the magnetic ordering. The intensity at twice this wave-vector is the first order multilayer structural Bragg peak. The dark areas represent the kinematical limits of the measurement. (b) The corresponding measurement in a saturation field of $H = 700 \text{ Oe}$. The AF correlations are suppressed leaving only the specular ridge ($Q_x = 0$) and the first order Bragg peak. The inset shows the specular reflectivity for the low (open symbol) and high (closed symbol) field data.

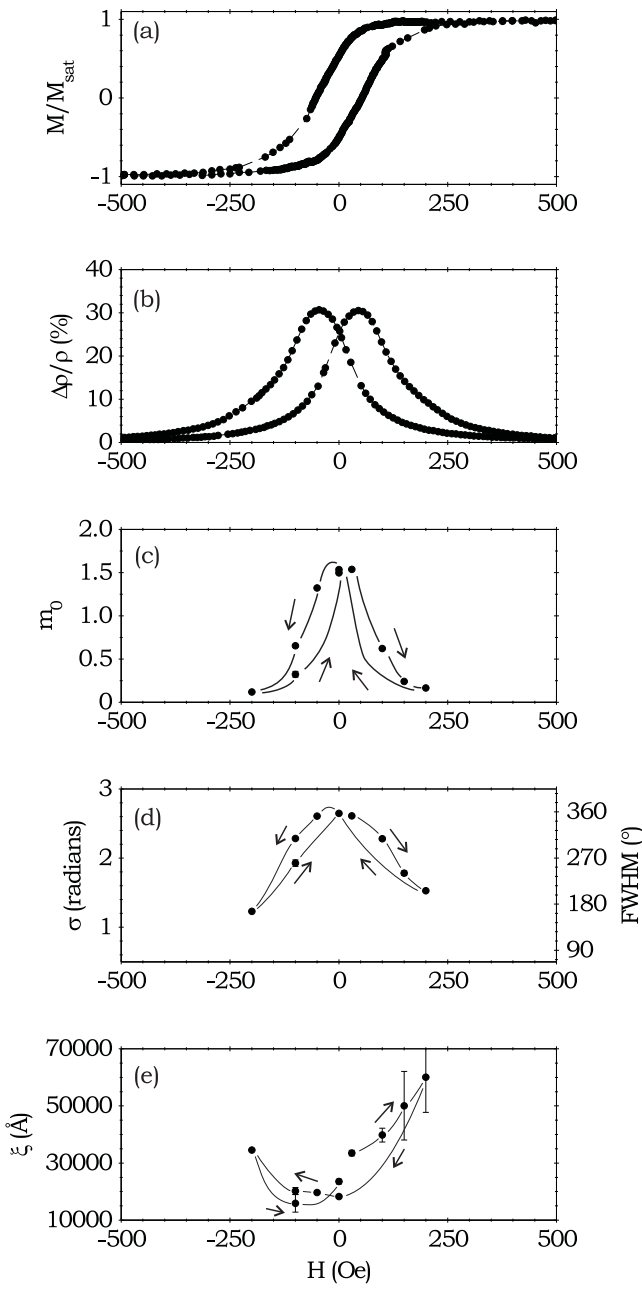


FIG. 2. The diffuse scattering observed at the AF peak as a function of applied field. Each scan is offset for clarity.

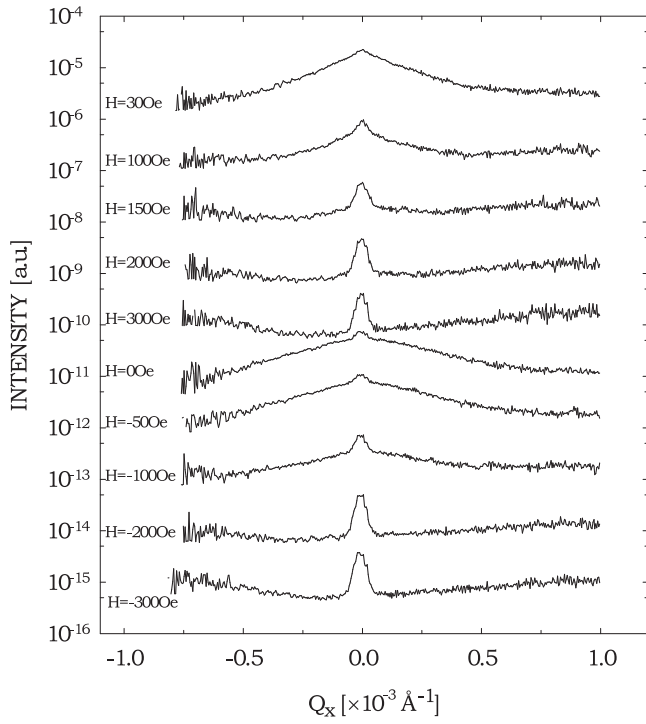


FIG. 3. (a): The room temperature MOKE magnetization loop for the $[Co(20\text{\AA})/Cu(20\text{\AA})] \times 50$ sample. (b) The magnetoresistance. Panels (c,d,e) represent the parameters described in the text. The lines are simply guides to the eye.